

Vibrational Heat Transport in Molecular Junctions

Dvira Segal and Bijay Kumar Agarwalla

*Chemical Physics Theory Group, Department of Chemistry,
University of Toronto, 80 St. George Street Toronto, Ontario, Canada M5S 3H6*

We review studies of vibrational energy transfer in a molecular junction geometry, consisting of a molecule bridging two heat reservoirs, solids or large chemical compounds. This setup is of interest for applications in molecular electronics, thermoelectrics, and nanophonics, and for addressing basic questions in the theory of classical and quantum transport. Calculations show that system size, disorder, structure, dimensionality, internal anharmonicities, contact interaction, and quantum coherent effects, are factors that interplay to determine the predominant mechanism (ballistic/diffusive), effectiveness (poor/good) and functionality (linear/nonlinear) of thermal conduction at the nanoscale. We review recent experiments and relevant calculations of quantum heat transfer in molecular junctions. We recount the Landauer approach, appropriate for the study of elastic (harmonic) phononic transport, and outline techniques which incorporate molecular anharmonicities. Theoretical methods are described along with examples illustrating the challenge of reaching control over vibrational heat conduction in molecules.

CONTENTS

I. INTRODUCTION	2
II. EXPERIMENTS: FOCUS ON HEAT CONDUCTION IN ALKANE CHAINS	4
III. METHODOLOGIES: Harmonic Approximation and the Landauer Formula	6
A. Formalism	6
B. Applications	8
IV. METHODOLOGIES: Anharmonic Interactions	9
A. Self-Consistent Reservoirs	10
B. Non-equilibrium Green's Function Approach	10
1. Formalism	10
2. Application	11
C. Quantum Master Equation	12
1. Weak molecule-reservoir coupling: The Bloch-Redfield-Markov equation	13
2. Strong molecule-surface coupling: polaronic equations	14
D. Numerically-Exact Simulations	15
V. Conclusions	16
ACKNOWLEDGMENTS	16
References	16

I. INTRODUCTION

Achieving control over energy transfer at the molecular scale is essential for the realization of molecular-based technologies. Good thermal conductors are desired in electronic applications where it is necessary to efficiently remove excess heat generated by electronic heat dissipation [1–3]. On the other hand, materials which are poor conductors of heat are required for the design of efficient thermoelectric devices [4, 5]. Intramolecular vibrational energy redistribution (IVR) and intermolecular vibrational energy transfer are central processes in chemistry, fundamental to our understanding of chemical dynamics, specifically, reaction rates [6, 7]. Moreover, in biomolecules, energy transfer processes determine stability, function, and regulation [8].

In this review, motivated by progress in probing heat transfer at the nanoscale, particularly, in self-assembled monolayers (SAMs) and nanostructured materials [9], we focus on the problem of vibrational heat flow through molecular junctions. After the presentation of representative experimental results, we describe quantum mechanical-based methodologies for the simulation of vibrational energy flow, focusing on the behavior of a single molecule. In the generic setup of interest a molecule is placed between two macroscopic contacts, labeled by L and R , see Fig. 1(a) for a schematic illustration. These thermal baths are characterized by well-defined thermodynamic properties, essentially, their temperatures T_L and T_R , potentially creating large biases, $(T_L - T_R)/(T_L + T_R) \sim 1$. Considering transport of vibrational energy in the junction, basic quantities of interest are the heat current j_q and the thermal conductance $\kappa \equiv j_q/\Delta T$ (units W/K) with $\Delta T = T_L - T_R$ as the temperature difference between the bulk objects. Complementary to solid/molecule/solid junctions, heat transfer in molecular chains can be studied in a “bridged” configuration, by connecting a molecule at its two ends to relatively large side groups which act (approximately) as thermal baths, see Fig. 1(b) for a scheme following Ref. [10]. In such experiments, a short laser pulse is applied to heat one end of the extended molecule. The heat transfer rate is then identified from optical-spectroscopy means, by measuring either the rate of energy loss from the excited unit, or energy gain at the other end.

Besides its relevance to technologies such as molecular electronics [11, 12], phononics [13, 14], thermoelectrics [5], spin caloritronics [15], Nanoelectromechanics [16], quantum optomechanics [17] and quantum information processing with hybrid quantum circuits [18], the generic model displayed in Fig. 1(a) is of basic interest for probing open quantum systems phenomena. Energy transfer processes in molecular junctions involve many-body interactions and quantum effects in a non-equilibrium situation, thus the setup can be employed to address fundamental questions in statistical mechanics, condensed matter physics, thermodynamics, and classical and quantum mechanics. Is energy transport in a given system ballistic or diffusive? What are the roles of many-body interactions in determining transport characteristics, especially when the system is driven beyond linear response? What are the signatures of quantum effects in molecular-scale heat transport? Can we design or predict a certain functionality from the model

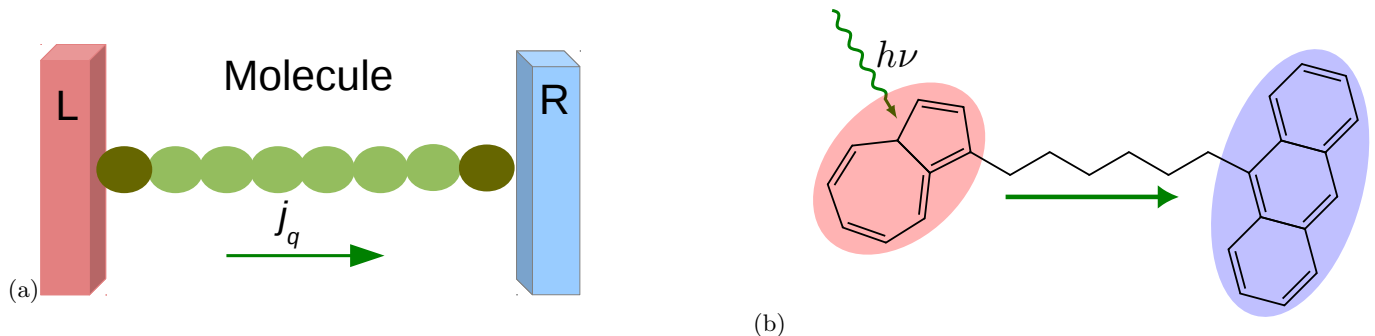


FIG. 1: (a) Scheme of a molecular junction consisting of two solids (possibly made of different materials, gold and quartz) and a molecule of several units, typically functionalized at its ends to improve chemical bonding with the solids, e.g., alkane-thiols of N units. Heat current is flowing from the hot reservoir (e.g., the left one) to the other-cold side. (b) Vibrational energy flow in molecules can be measured using pump-probe laser spectroscopy tools, in liquid solutions at ambient temperatures. In this illustration, the molecule of interest (alkane chain) is connected at its two ends to large molecular groups acting as local heat reservoirs, for example, azulene and anthracene [10]. The azulene group is excited optically. The time for intramolecular vibrational energy transfer, through the bridge to the anthracene unit, is measured for different chain lengths, to identify the dominant transport mechanism.

Hamiltonian? Other questions (not reviewed here), which have attracted significant attention, concern the emergence of the phenomenological-macroscopic Fourier’s law of heat conduction from first principles (classical and quantum) [19], and the derivation of sufficient or necessary conditions for realizing negative differential thermal conductance and thermal rectification [13, 14, 20]. The latter effect, also referred to as the thermal diode effect, features junctions in which the magnitude of the thermal current depends on the direction (polarity) of the temperature difference.

In this review our main focus are theoretical frameworks for the calculation of vibrational energy flow in molecular junctions, and we contain ourselves to quantum mechanical treatments. Why concern with quantum effects? Molecular vibrational frequencies typically extend room temperature, $\hbar\omega > k_B T$, thus the quantum statistics is important; in classical simulations the average energy per phonon mode is $k_B T$, with k_B as the Boltzmann constant, resulting in an overestimate of e.g., the specific heat (thus the thermal conductivity), since $\frac{\hbar\omega}{e^{\hbar\omega/k_B T} - 1} < k_B T$.

Because of the wide scope of the field of heat transfer, we leave out many interesting topics which were covered in recent reviews. Concepts, experiments, and computational approaches in nanoscale thermal transport were recently organized into several comprehensive works [9, 14, 21, 22], with a focus on low-dimensional nanostructured materials such as graphene, carbon nanotubes, and Si nanowires, rather than molecular-level transport. Other relevant reviews cover control over energy dissipation at the nanoscale [1], advances in thermoelectrics of semiconductor nanostructured materials [5], studies over the nature of vibrational energy flow in proteins [8], and heating, heat transfer, and thermoelectricity at the nanoscale [23]. Concerning methodologies for calculating nanoscale phonon transport, recent reviews detailed classical simulations [19, 24, 25] and quantum-mechanical methodologies [19], specifically Green’s function-based approaches [26–28]. Other studies featured phononic devices [13, 14] and phonon-assisted effects in molecular electronic conduction [29]. Obviously, the interaction of electrons with phonons is intrinsic for both charge and energy transfer processes in molecular systems [30]. Here we simplify the problem considerably by studying only the dynamics of vibrational-nuclear degrees of freedom. Even under this separation, the situation depicted in Fig. 1 is deeply complex given the interplay of quantum effects, many-body (phonon-phonon) interactions, far-from-equilibrium driving, and the diversity in molecular structures and contact geometries.

Before discussing experimental results and theoretical methodologies, it is useful to recall two central-limiting energy transfer mechanisms which are well defined in macro-to-mesoscale systems: ballistic and diffusive. Ballistic transport corresponds to direct point-to-point propagation of energy, obeying the scaling $l \propto t$, with t as the traveling time to cross the distance l . It shows up in ordered structures in which the mean free path, the average distance traveled by phonons between successive scattering events, is larger than the size of the conductor. This is the case e.g., in some (up to μm -length) nanotubes [3], and more relevant to our review, alkane chains of 5-25 units, at room temperature [10, 31–36]. Diffusive energy transport is a multiple-step process, with energy “hopping” between sites, obeying the scaling $l \propto \sqrt{t}$. It is observed in bulk systems and disordered structures, e.g., peptides [8, 37], glasses, amorphous and doped nanostructures [9].

The distinction between ballistic and diffusive dynamics, and the notion of a mean free path, are natural to macro-scale and nanostructured systems, but in relatively short molecules as considered below (5-50 Å) these concepts

are not well defined. Instead, in the molecular realm we distinguish between harmonic models, assuming atomic displacements follow Hooke’s law, and anharmonic cases, allowing for anharmonicities in the molecular force field. In harmonic models the current may show ballistic characteristics, with the conductance determined by the contacts only, or, “phonon tunneling”, when phonons off-resonance with molecular vibrations, cross the junction, showing features of quantum tunneling [38]. We use Eq. (12) below to exemplify the concepts of ballistic and tunneling phonon dynamics in molecular heat conduction. Note that we use the notions of phonons and vibrations interchangeably, referring to the collective motion, excitations, of atoms.

II. EXPERIMENTS: FOCUS ON HEAT CONDUCTION IN ALKANE CHAINS

We begin with the presentation of several experiments, corresponding to the schemes in panels (a) and (b) of Fig. 1. This introduction serves to motivate modeling and computational works, but it does not aim to give readers a complete review over heat transfer measurements, provided e.g. in Refs. [9, 21]. We focus on studies of length-dependent thermal transport in alkane chains with 2-25 methylene units. This molecule serves as a standard for phononic transport measurements for several reasons. First, these sigma-bond hydrocarbons are poor conductors of electricity, therefore thermal conduction takes place by phonons, not electrons. Second, the molecule is uniform and quasi one-dimensional. Lastly, at room temperature anharmonic effects are expected to be non-influential even in long chains of $N \sim 100$ units [38]. Altogether, alkane chains with $N \gtrsim 5$ units are expected to conduct vibrational energy ballistically at room temperature, as confirmed by simulations [38] and experiments [10, 31–36].

Solid-SAMs-solid junctions were studied in several works. The thermal conductance of Au-alkanedithiol-GaAs SAMs with 8-10 carbon units was measured in Ref. [31] with a 3ω technique, resulting in the room-temperature value (per unit area) of $\kappa \sim 25 - 28 \text{ MW m}^{-2} \text{ K}^{-1}$, independent of length. More recently, heat transport measurements with scanning thermal microscopy (SThM) were reported in Ref. [32], with an alkane-thiol molecule adsorbed on a gold surface and a silicon tip approaching the SAM from above. The measured value for the thermal conductance is depicted in Fig. 2(b). It shows a non-monotonic behavior: The conductance first rises with length for short chains, with the maximum conductance of 25 pW/K for a chain with four carbon atoms, but in longer chains κ is reduced to ~ 10 pW/K. This crossover behavior appears in simulations, see Fig. 2(a), to be discussed in more details in Sec. III B.

In ballistic transport the conductance reflects the molecule-contact interaction rather than intrinsic molecular properties. The effect of chemical bonding on interfacial heat transport in Au/alkane SAMs/Quartz junctions was examined in Ref. [33], by studying chains with either methyl or thiol-termination, using the time-domain thermoreflectance (TDTR) technique, an optical pump-probe tool. The thiol-ending group forms a stronger (covalent) bond to the Au surface, relative to the weak (van der Waals) forces attaching a methyl group to a gold substrate. In accord with expectations, the interface thermal conductance was enhanced with the increase of bond strength: The interfacial thermal conductance (per unit area) measured for the thiol ending group was $\kappa=68 \text{ MW m}^{-2} \text{ K}^{-1}$. A lower value was reached for the interface missing thiol bonds, $\kappa = 36 \text{ MW m}^{-2} \text{ K}^{-1}$ [33]. In Ref. [39] it was also demonstrated experimentally that the thermal conductance of alkane SAMs can be systematically controlled-reduced by using metals with mismatched phonon spectra, e.g., Au and Pt.

Bridged-type situations as depicted in Fig. 1(b) were examined in several works, revealing information on mechanisms of heat flow from the dynamics of the transients. In one of the earliest studies, alkane chains were connected to large chromophores, azulene and anthracene, which effectively act as heat reservoirs [10]. The IVR process began by the electronic excitation of the azulene end-group, and after a fast internal conversion, vibrational energy localized on the azulene propagated through the bridge to the anthracene, with an IVR time constant of $\tau \sim 5 - 6$ ps. It was demonstrated that results were consistent with a ballistic transport model [10]. At later times, equilibration with the surrounding solvent took place.

A rather different approach, time-resolved flash-heating of SAMs on substrates, was utilized in Ref. [40], see also [34, 41]. In this type of experiments, a thin metal film (gold) was heated by several hundreds of degrees within a very short time (~ 1 ps) using a laser pulse, to excite electrons near the metal surface. Subsequently, the lattice temperature rose due to electron-phonon coupling, and heat propagated from the base of the SAM, through the molecular chains, to the top (methyl) groups where it was detected with vibrational sum-frequency generation (SFG) spectroscopy. This signal is sensitive to disorder on the SAM, induced here by the temperature increase, as well as to frequency shifts. By varying the length of the alkane chain it was determined that heat flew in alkanes ballistically, with a velocity of 9.5 \AA/ps , to yield a thermal conductance (per molecule) of 50 pW/K.

Other recent studies further considered a bridged setup in solution and confirmed the ballistic energy transport mechanism at room temperature in alkane chains of 5-15 units, by using two-dimensional infrared spectroscopy (2DIR) [35, 36]. In this experiment, the energy transfer process was initiated by vibrationally exciting a “tag” group attached to one end of the molecule (e.g. $\text{N}\equiv\text{N}$ bond), while the vibrational energy arriving at the other end was recorded by

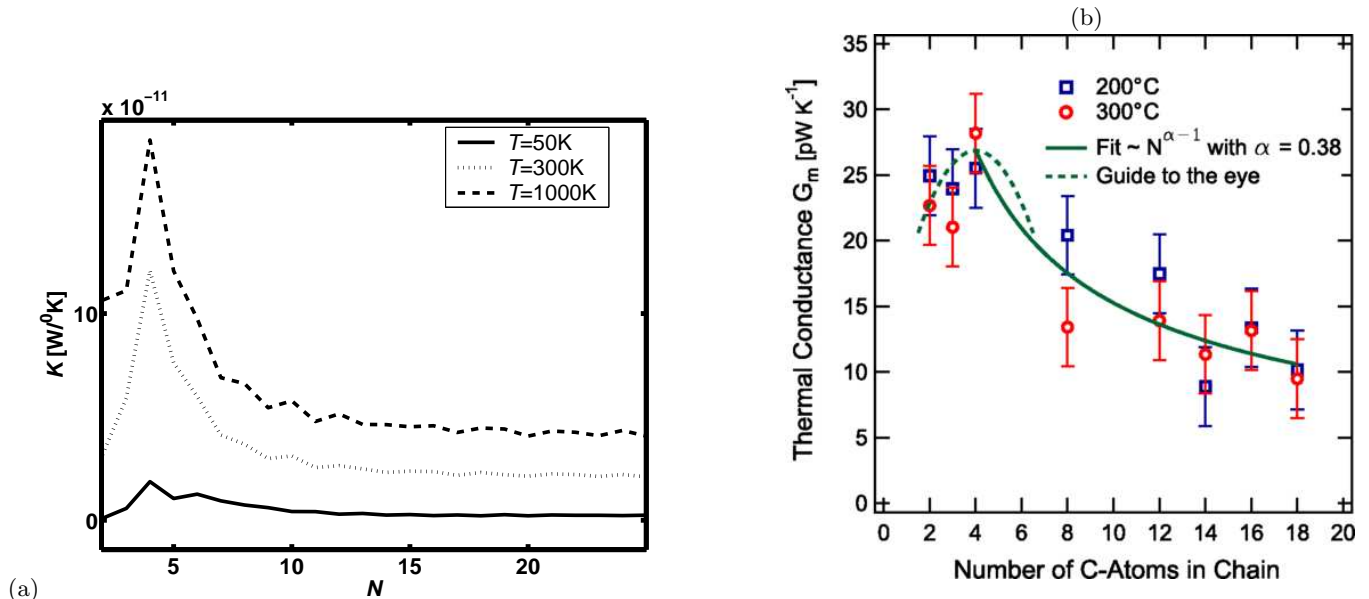


FIG. 2: Thermal conductance of alkane chains with increasing size. (a) Simulations under the harmonic approximation based on the Landauer formula, as reported in Ref. [38]. The reservoirs’ spectral functions are modeled by $\gamma(\omega) = \frac{a}{\hbar} e^{-\omega/\omega_c}$, identical for L and R , with Debye (cutoff) frequency $\omega_c = 0.05$ eV and a coupling energy $a = 1$ eV. Full line: $T=50$ K; dotted line: $T = 300$ K; dashed line: $T=1000$ K. (b) Measured values for the thermal conductance of SAMs of alkane thiols $[\text{HS}-(\text{CH}_2)_{N-1}-\text{CH}_3]$ on gold substrates on Mica, using SThM with a silicon tip. Panel (b) is reprinted with permission from Reference [32]. Copyright 2014 American Physical Society.

a “reporter” group, e.g., a carbonyl. Measurements at room temperature, in solution, revealed fast energy transport through alkanes with a speed of $14.4 \text{ \AA}/\text{ps}$ and a mean free path of 14.6 \AA , see Fig. 3. Interestingly, while it was demonstrated that transport via the chain was ballistic, it was argued that heat propagated through the end-groups in a diffusive manner [35]. It was also demonstrated in Ref. [42] that by initiating dynamics with different tags, different chain bands (e.g., CC stretching, CH_2 twisting modes) contribute to the transfer process.

Thermal transport experiments on hydrocarbons confirmed ballistic dynamics, the predominant mechanism in short-ordered systems. In contrast, diffusive dynamics is prevalent in complex systems (even of reduced dimensions), nanotubes and nanowires [3, 22, 43], polymers [9], peptides [8, 37], as well as in small organic molecules [36]. For example, in Ref. [37] diffusive transport of vibrational energy was observed in short 3_{10} -helical peptides. The process was initiated by depositing excess energy e.g. onto a vibrational CD mode. Flow of energy through the helix was then detected optically by planting vibrational probes, isotopically-labeled CO modes, in several locations away from the source, serving as local thermometers. Measurements in Ref. [37] were consistent with a diffusion model, with a diffusivity constant of $2 \text{ \AA}^2/\text{ps}$ [44].

In the following discussion over theoretical-computational frameworks we do not direct the issue of the ballistic-diffusive crossover in thermal conduction, as diffusive dynamics is not expected to fully develop in short molecular junctions, our focus here. More generally though we will evaluate the role of nonlinearities, deviations from the harmonic approximation for atomic displacements, in the heat transport behavior. What are the signatures of anharmonicities in relatively small phononic conductors? First, one may observe the suppression of the thermal conductance with temperature, at high temperatures, when inelastic phonon scattering effects are at play [45]. Further, anharmonicities can furnish nonlinear functionalities such as the thermal diode effect [13, 46, 47], which is specifically predicted to develop in the azulene-alkane-anthracene compound of Fig. 1(b) at high temperatures [48]. Other distinct signatures of vibrational anharmonicities are processes such as energy localization and unidirectional energy flow in molecules. Using IR Raman spectroscopy, it was manifested that in nitrobenzene vibrational energy could leave benzene-localized modes to occupy global modes, but energy could not propagate away after a nitro excitation [49–51]. Asymmetries in forward-backward transfer efficiencies certainly break the noninteracting phonon picture. We describe now quantum mechanical approaches for modelling vibrational energy flow in molecular junctions.

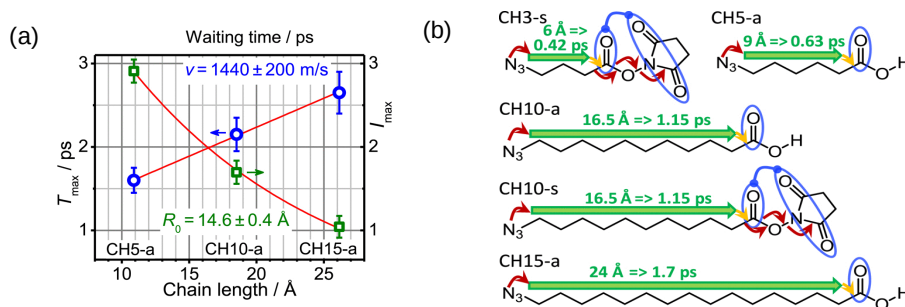


FIG. 3: Two-dimensional IR spectroscopy of vibrational energy transfer in alkanes. (a) Inferred energy transport time T_{max} , from the tag mode to the reporter, and the tag-reporter cross-peak maximum amplitude I_{max} , plotted as a function of chain length. The behavior of T_{max} is approximated by a linear function, and from the (inverse) slope one receives the speed ~ 14.40 Å/ps. The cross peak amplitude is approximated by an exponentially decaying function with a characteristic decay distance $R_0 \sim 14.6$ Å, representing the mean free path. (b) Schemes of energy transport mechanisms in alkane chains with different reporter groups (blue). Green arrows mark regions of ballistic propagation, red arrows mark (diffusive) steps from the tag group to the molecule, and from the molecule to the reporter. Yellow arrows point to the relaxation of the vibrational wavepacket. Also indicated are ballistic transport times, computed from the chain length divided by the energy transport speed 1440 m/sec. Reprinted with permission from Reference [35]. Copyright (2015), AIP Publishing LLC.

III. METHODOLOGIES: HARMONIC APPROXIMATION AND THE LANDAUER FORMULA

A. Formalism

Under the harmonic approximation for atomic displacements, the molecule (“subsystem”) includes harmonically-connected masses, and it is linked linearly-harmonically to thermal environments composed of harmonic oscillators (“baths”). Since all terms are harmonic, one can diagonalize the model Hamiltonian to reach its fundamental normal modes (phonons) and solve the dynamics of this noninteracting problem exactly. The steady state transport behavior of the model can be arrived at by using different methods, including the generalized Langevin equation [19, 38, 52–54] or, equivalently, the non-equilibrium Green’s function (NEGF) approach [26, 28, 55] (derivations under the weak-coupling approximation can be found e.g., in Ref. [56].) Both methods yield a Landauer-type formula for the heat current, an analogue of the elastic-coherent expression for charge current [57].

Following Refs. [19, 38, 53], we outline the derivation of the Landauer heat transport expression from the principles of the Langevin equation approach. In this procedure, one begins with Heisenberg equations of motion for displacement and momentum operators, assuming a system-bath factorized initial condition at $t = -\infty$ with the reservoirs prepared in a thermodynamic equilibrium. It can be shown that after integrating out the baths’ coordinates, the subsystem’s displacements follow a generalized (quantum) Langevin equation in which the effect of the reservoirs is encapsulated within dissipation kernels and noise terms. These terms particularly depend on the baths’ spectral properties. Fourier transforming the generalized Langevin equation administers the steady state limit. In frequency domain, the linear equations for molecular coordinates can be readily solved to construct two-time correlation functions, to organize a closed-form expression for the heat current, a Landauer-type formula [19, 38, 53]. For harmonic models, the quantum Langevin equation and the NEGF method can be further employed to yield closed expressions for the fluctuations of the heat current [58, 59].

We now provide the working expressions. The Hamiltonian for a harmonic junction reads

$$H = H_S + H_L + H_R + H_I, \quad (1)$$

where the molecule H_S , the two contacts H_ν , $\nu = L, R$, and the coupling term H_I are written as

$$\begin{aligned} H_\alpha &= \frac{1}{2} p_\alpha^T p_\alpha + \frac{1}{2} u_\alpha^T K_\alpha u_\alpha, \quad \alpha = S, L, R \\ H_I &= \sum_{\nu=L,R} u_\nu^T \Lambda_{\nu S} u_S. \end{aligned} \quad (2)$$

The vector $u_\alpha = \sqrt{m_\alpha} x_\alpha$ gathers mass-normalized displacement operators for the three regions $\alpha = L, R, S$. Similarly, p_α holds the conjugate momenta, T stands for matrix transpose. The force constants are organized into real symmetric

matrices K_S , K_L and K_R , and the harmonic (separable) interaction of the molecule with the two reservoirs is given in terms of the force constant matrices $\Lambda_{LS} = [\Lambda_{SL}]^T$ and $\Lambda_{RS} = [\Lambda_{SR}]^T$. Note that in general one does not need to assume a normal mode representation for the reservoirs as this may be achieved through diagonalization with unitary matrices U_ν ,

$$U_\nu^T K_\nu U_\nu = \Omega_\nu^2. \quad (3)$$

In steady state, the phonon current across harmonic junctions is given by a Landauer-type expression [60]

$$j_q = \frac{1}{2\pi} \int_0^\infty d\omega \hbar\omega \mathcal{T}(\omega) [n_L(\omega) - n_R(\omega)]. \quad (4)$$

Here, $n_\nu(\omega) = [e^{\beta_\nu \hbar\omega} - 1]^{-1}$ are Bose-Einstein distribution function for the $\nu = L, R$ bath with the inverse temperature $\beta_\nu = 1/(k_B T_\nu)$, $\mathcal{T}(\omega)$ stands for the transmission function calculated from [19, 61]

$$\mathcal{T}(\omega) = \text{Tr}[G_0^r(\omega)\Gamma_L(\omega)G_0^a(\omega)\Gamma_R(\omega)]. \quad (5)$$

For small temperature differences, $\Delta T \ll T$ with $\Delta T \equiv T_L - T_R$, $T = (T_L + T_R)/2$ as the average temperature, the Landauer expression reduces to

$$j_q = \frac{\Delta T}{2\pi} \int_0^\infty d\omega \hbar\omega \mathcal{T}(\omega) \frac{dn(\omega)}{dT}, \quad (6)$$

with $n(\omega)$ as the Bose-Einstein function at the averaged temperature T . The ingredients in Eq. (5) are the Green's function of the molecule, $G_0^r(\omega) = (G_0^a(\omega))^\dagger$, and its self energy,

$$\begin{aligned} G_0^r(\omega) &= [(\omega + i0^+)^2 - K_S - \Sigma_L^r(\omega) - \Sigma_R^r(\omega)]^{-1}, \\ \Sigma_\nu^r(\omega) &= [\Lambda_{\nu S}]^T g_\nu^r(\omega) \Lambda_{\nu S}, \quad \Gamma_\nu(\omega) = i[\Sigma_\nu^r(\omega) - \Sigma_\nu^a(\omega)], \quad \nu = L, R \end{aligned} \quad (7)$$

where $\Gamma_\nu(\omega)$ is referred to as the spectral function for the leads. The unperturbed-isolated Green's function for the baths are given by

$$g_\nu^r(t) = -\theta(t) U_\nu \frac{\sin(\Omega_\nu t)}{\Omega_\nu} U_\nu^T, \quad g_\nu^r(\omega) = \int_{-\infty}^\infty e^{i\omega t} g_\nu^r(t) dt = [(\omega + i0^+)^2 - K_\nu]^{-1}, \quad (8)$$

with $\theta(t)$ as the Heaviside step function. The Landauer equation (4) relies on the harmonic approximation, yet even under this strong assumption it can be employed to address a broad range of problems: the behavior of heat conduction in one-dimensional chains, as opposed to the three-dimensional case, the role of disorder in thermal transport, as well as impurities, molecular structure (linear or T-shaped objects), reservoir's spectral properties, and contact geometry.

We now specify Eq. (2) and introduce a chain model with the first (last) atoms in the chain coupled to the left (right) baths,

$$H = H_S + \sum_{l \in L} \left[\frac{p_l^2}{2} + \frac{1}{2} \omega_l^2 \left(u_l - \frac{\lambda_l u_1}{\omega_l^2} \right)^2 \right] + \sum_{r \in R} \left[\frac{p_r^2}{2} + \frac{1}{2} \omega_r^2 \left(u_r - \frac{\lambda_r u_N}{\omega_r^2} \right)^2 \right]. \quad (9)$$

The small-letter parameters, λ , $\omega_{l,r}$, are elements in the matrices Λ , and Ω_ν , respectively. The self energy matrices reduce to single elements, e.g., at the left contact

$$[\Sigma_L^r(\omega)]_{n,n'} = \Sigma_L^r(\omega) \delta_{n,n'} \delta_{n,1} = - \int_0^\infty e^{i\omega t} \sum_{l \in L} \lambda_l^2 \frac{\sin(\omega_l t)}{\omega_l} dt. \quad (10)$$

The real part of the self energy presents frequency shifts to molecular modes, the result of the coupling to the bath. The imaginary part of the self energy is responsible for energy damping. Ignoring frequency shifts, it is convenient to express it in terms of a (real-valued) function $\gamma_\nu(\omega)$, defined from $\Sigma_\nu^r(\omega) \equiv -i\omega\gamma_\nu(\omega)$. It corresponds to the friction coefficient in the language of the quantum Langevin equation.

Simulations of phononic heat current based on Eq. (4) are feasible, but analytic results are limited to special cases, e.g, to the classical-high temperature limit of a uniform chain [19], or to short atomic bridges [62]. To provide insights into the transport behavior, we exemplify Eq. (4) in the single-atom limit, taking into account a single oscillator which is directly coupled to the L and R reservoirs. We denote the frequency of this mode by ω_0 adhering to the notation employed in the literature, see e.g. Refs. [63, 64]. The transmission function of this bridge is given by

$$\mathcal{T}(\omega) = \frac{4\omega^2 \gamma_L(\omega) \gamma_R(\omega)}{(\omega^2 - \omega_0^2)^2 + \omega^2 [\gamma_L(\omega) + \gamma_R(\omega)]^2}, \quad (11)$$

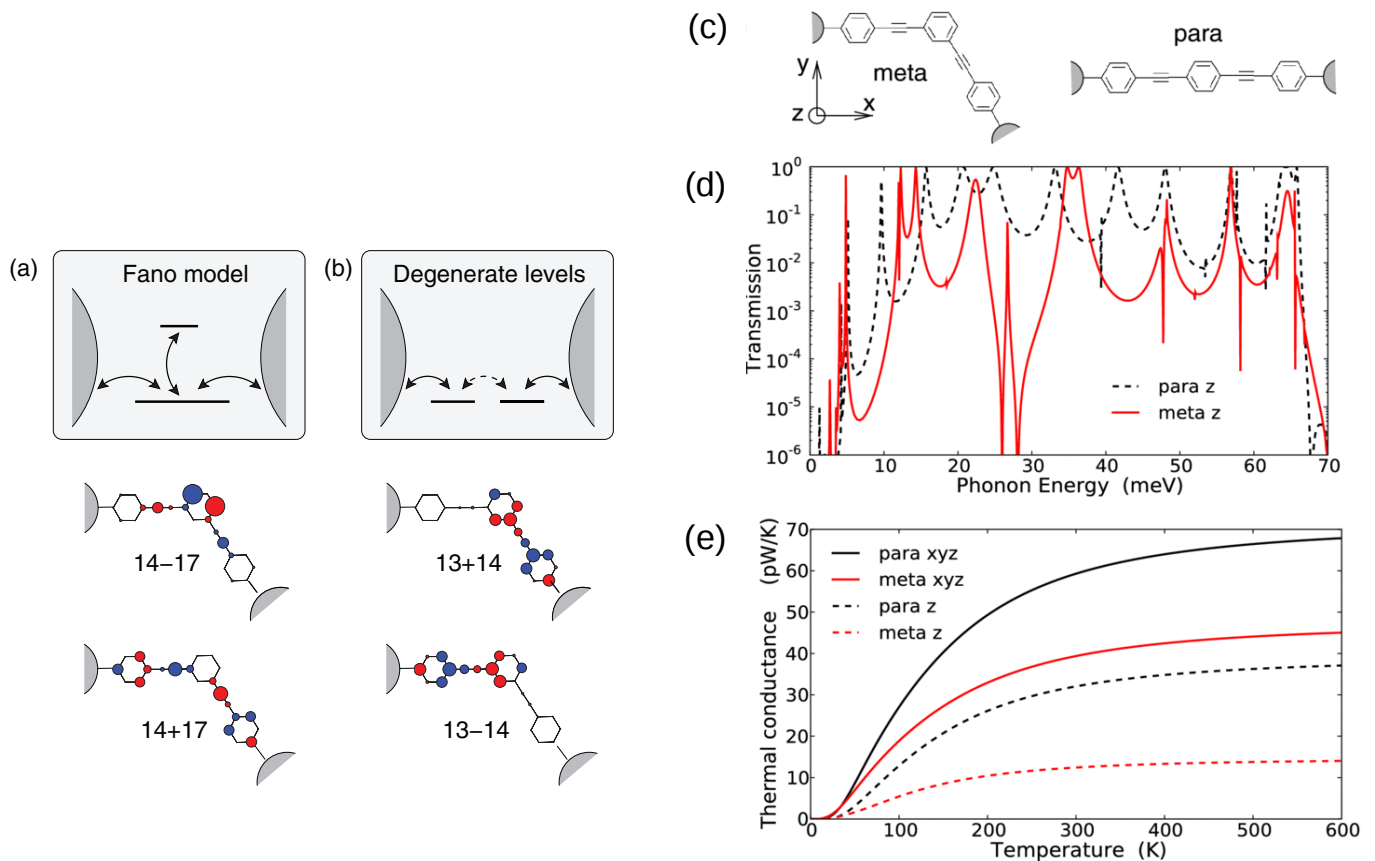


FIG. 4: Quantum interference effects of phononic conduction in molecular junctions. (a)-(b) Examples of localized phonon modes (linear combinations of normal modes) in oligo(phenylene-ethynylene) (OPE3), a cross conjugated molecule. Numbering counts the eigenmodes. The modes may behave similarly to the Fano model (a) or the degenerate-levels model (b). (c) meta and para OPE3 configurations, (d) calculated transmission functions, and (e) the thermal conductance, considering out-of-plane modes only (z) or the complete spectrum involving (x, y, z) displacements. Reprinted with permission from Reference [70], Copyright (2013), AIP Publishing LLC.

and the phonon current through the junction is

$$j_q = \frac{2}{\pi} \int_0^\infty d\omega \hbar \omega \frac{\omega^2 \gamma_L(\omega) \gamma_R(\omega)}{(\omega^2 - \omega_0^2)^2 + \omega^2 [\gamma_L(\omega) + \gamma_R(\omega)]^2} [n_L(\omega) - n_R(\omega)], \quad (12)$$

see also Refs. [62, 65] (albeit adopting a different notation). This simple expression describing quantum coherent transport allows us to clarify several concepts: (i) When incoming phonons are in resonance with the molecular mode, $\omega = \omega_0$, the transmission is only limited by contact effects. We refer to this type of motion as “ballistic” transport. Furthermore, in the ideal case with a perfect transmission, $\mathcal{T}(\omega) = 1$, we evaluate the conductance from (6) and receive $\kappa = \frac{1}{2\pi} \int_0^\infty d\omega \hbar \omega \frac{dn}{dT} = k_B^2 \pi^2 T / 3h$, which is the (universal) quantum of thermal conductance [55, 60, 66, 67], confirmed experimentally in Ref. [68]. (ii) The damping function γ_ν , resulting from the molecule-bulk coupling, broadens the resonance allowing for “tunneling” of phonons, transmission of modes off-resonance with the molecular frequency, $\omega \neq \omega_0$. It can be shown that the tunneling contribution exponentially decays with bridge-length [38], in analogy with the super-exchange mechanism of electron transfer [69]. (iii) The conductance grows with T at low temperatures, but once $k_B T > \hbar \omega_0$, it saturates as it approaches the classical limit.

B. Applications

The transmission function (5) can be evaluated using the so-called atomistic Green’s function approach [28] to provide the thermal conductance of a broad range of nanoscale objects, carbon nanotubes, Si nanowires, graphene sheet, graphite. In such calculations one typically computes the phonon dispersion based on a model for the interatomic

potential, then evaluates the transmission function employing a model for the self energies. Phonon transport in carbon nanotubes was examined in e.g. Refs. [71, 72] using this analysis.

We discuss now examples of Landauer-based calculations of heat transfer in relatively short molecules. Alkane chains and isotopically substituted disordered chains with 2-25 units were examined in Ref. [38], showing the conductance to exhibit non monotonic features at room temperature with growing size, see Fig. 2(a). This behavior results from the fact that the molecular vibrational spectrum may be largely altered with length for short molecules, as well as the degree of localization of some molecular normal modes. Since details of the molecule-heat baths (solids) coupling, the spectral properties of the solids, specifically the value of their Debye frequency, and the bulk temperature, determine which molecular modes participate in the conduction process, the conductance of ultra-small systems can be tuned with size, before ballistic motion takes over [38]. Fig 2(a) displays results at different temperatures assuming ohmic thermal baths. Panel (b) depicts measurements of the thermal conductance in SAMs [32], demonstrating a qualitative agreement in trends between theory and experiment.

Reducing phononic heat conductance in molecular junctions (while maintaining high electronic conductance), is desirable for improving thermoelectric efficiency. Several design principles for molecules were tested in recent proposals, bringing modest success, as we discuss below. The challenge in the manipulation of phononic current is rooted in the bosonic statistics: Technically, if we replace the bosonic form in Eq. (6) by the corresponding fermionic function, the current would be determined by the transmission function only in the vicinity of the equilibrium Fermi energy. For molecular structures, the charge current then combines contributions from a single or few resonance levels. In contrast, the derivative of the Bose-Einstein distribution function in Eq. (6) covers frequencies in a window up to the baths' temperatures, potentially comprising substantial contributions from many molecular modes of different nature, localized and extended, to confuse dynamics.

In Ref. [73] it was proposed that molecules made of two separate subunits with a weak chemical link, for example, π -stacked aromatic rings, could show reduced thermal conductance relative to the case with a single unit, while maintaining good electrical conductivity (since electronic overlap through-space is preserved in π - π systems). Detailed simulations with first-principle parameters revealed a more intricate picture: The phonon conductance may indeed reduce (by about a factor of 2) in this design, relative to the case with a single unit, but in some cases, it *increased* due to an overall improvement of coupling in the junction.

Reduction of thermal conductance in molecules by employing the effect of quantum interference was demonstrated in Ref. [70]. It was pointed out that in e.g. a benzene ring with a meta connection to the leads, the phononic transmission function (comprising in-plane vibrations) can exhibit destructive quantum interference features, resulting in the suppression of the thermal conductance compared to the linearly conjugated analogue, see Fig. 4. This behavior is conceptually similar to the electronic case [74, 75]. However, while variations in electronic conductance due to interference effects may be of 1-3 orders of magnitude [74, 75], changes in phononic conductance due to quantum interference are rather modest, factor of 1.5 to 5 in Ref. [70]. As explained above, this is because phononic conductance collects contributions from many modes of different nature, whereas quantum interference effects influence individually specific modes.

IV. METHODOLOGIES: ANHARMONIC INTERACTIONS

The Landauer picture breaks down when deviations from the noninteracting normal-mode picture are significant. This is the case in systems with large-tunable anharmonicity [as in the FPU model [76]] and at high temperatures when inelastic phonon scatterings are influential. What tools are available beyond the Landauer-harmonic approach? Classical molecular dynamic simulations can be naturally applied beyond harmonic force fields, to include interactions to all orders [24, 25, 77, 78]. Molecular dynamics simulations of heat conductance in simplified models revealed the role of disorder and reduced dimensionality [79–81] as well as anharmonicities [82–86] on transport mechanisms and the occurrence of nonlinear phenomena such as negative differential thermal conductance [87], thermal rectification [88, 89], gating [90], and memory elements [91].

Quantum mechanical treatments are typically limited to a certain range in parameters. Among relevant methods we mention the non-equilibrium Green's function technique, which is perturbative in the nonlinear interaction strength [27, 28], and master equation approaches, which may include the effect of anharmonicity exactly (as long as the model is minimal), but are often limited to models with weak system-bath couplings [45, 63, 92]. Other schemes are based on time-scale separation between slow and fast modes [93], phenomenological self-consistent treatments [19, 53, 94, 95], and numerically-exact methodologies, computationally limited to minimal modes [96–98].

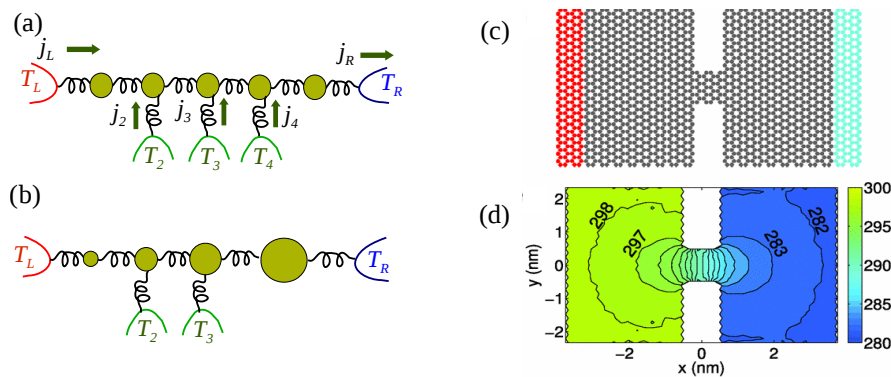


FIG. 5: (a) Illustration of the SCR model in a chain model with $N = 5$ atoms. Under the self consistent conditions, $j_L = j_R$. The conditions $j_2 = j_3 = j_4 = 0$ set the temperatures T_i , $i = 2 - 4$. (b) An example of a spatially asymmetric model (the different sizes reflect different masses), which realizes a thermal diode effect - only in the quantum regime [94]. (c) Graphene nano constriction and (d) its self-consistent temperature profile (K) in the quantum SCR model. Temperatures were determined self-consistently for the gray atoms in the central region. A classical approximation provided very similar results. Panels (c) and (d) are adapted with permission from Ref. [95].
Copyrighted 2013 American Physical Society.

A. Self-Consistent Reservoirs

The self-consistent reservoir (SCR) method introduces effectively anharmonic interactions into harmonic models by allowing the system to exchange energy with internal reservoirs which mimic many-body interactions. In Fig. 5(a)-(b) we exemplify the model with a one-dimensional chain. The system includes N atoms (not necessarily identical) in a junction setting, connected to each other by harmonic springs. In addition, each particle is coupled to an independent harmonic (Langevin) thermal reservoir, also referred to as a “thermal Büttiker probe” [99]. The temperatures at the “exterior” reservoirs, attached to the first and last particles, are set at T_L and T_R , but the temperatures of the internal baths are determined in a self consistent manner, by demanding that in steady state, on average, there is no net heat current from these baths to the physical system.

The SCR model has been investigated intensively with toy models. It was originally proposed in the classical domain [100, 101], to prove the emergence of diffusional dynamics and Fourier’s law of heat conduction upon the application of the interior reservoirs [102]. The model was later extended to describe heat conduction in quantum systems, in linear response [19, 103, 104] and beyond that, analytically-approximately [105, 106], and numerically-exactly [94, 95]. What are the signatures of anharmonicity within the SCR model? The interior reservoirs can gradually tune the transport dynamics, from ballistic-elastic to diffusive. Further, the quantum SCR method can support a diode behavior (which is identically missing under the Landauer expression, as well as in the classical SCR method), due to the interplay of quantum effects, spatial asymmetry, and effective anharmonicity, see a possible setup in Fig. 5(b) following Ref. [94].

Beyond toy models, the SCR method has been recently applied in Ref. [95] for the study of quantum thermal transport in nanostructures such as the two-dimensional graphene constriction depicted in Fig. 5(c). The temperature profile in the central region was evaluated with a quantum SCR treatment, displayed in Fig. 5(d). Interestingly, it was found that the quantum profile closely matches classical results, suggesting that low-frequency modes, for which quantum and classical statistics agree, largely contribute to transport in this system.

In conclusion, while missing genuine anharmonic interactions, the SCR method offers a simple mean for studying phononic conduction in nanostructures while including both quantum effects and (effective) inelastic phonon scatterings.

B. Non-equilibrium Green’s Function Approach

1. Formalism

The non-equilibrium Green’s function technique offers an elegant-powerful mean for computing equilibrium and out-of-equilibrium properties of many-body systems [107–110]. For quantum transport problems, the NEGF approach

provides a computational framework for incorporating interactions (anharmonicities, in the heat transport problem), going beyond the Landauer expression. We begin by introducing the Meir-Wingreen formula for the steady state heat current flowing through an anharmonic system which is linearly (harmonically) coupled to two harmonic reservoirs L and R [27, 110–112],

$$j_q^L = \frac{1}{2\pi} \int_0^\infty d\omega \hbar\omega \text{Tr}[G^<(\omega)\Sigma_L^>(\omega) - G^>(\omega)\Sigma_L^<(\omega)]. \quad (13)$$

Here, $\Sigma_\nu^<(\omega) = -in_\nu(\omega)\Gamma_\nu(\omega)$ and $\Sigma_\nu^>(\omega) = -i[1 + n_\nu(\omega)]\Gamma_\nu(\omega)$, are the self-energy components for $\nu = L, R$. The harmonic part of the Hamiltonian was described in Sec. III A. Adding nonlinear terms to H_S , the molecular Green's function G now incorporates anharmonicities. One can formally write down a closed set of equations for its components in terms of the nonlinear self-energy Σ_n ,

$$\begin{aligned} G^r &= [(G_0^r)^{-1} - \Sigma_n^r]^{-1} = [(\omega + i0^+)^2 - K_S - \Sigma_L^r - \Sigma_R^r - \Sigma_n^r]^{-1}, \\ G^{<,>} &= G^r (\Sigma_L^{<,>} + \Sigma_R^{<,>} + \Sigma_n^{<,>}) G^a. \end{aligned} \quad (14)$$

For simplicity, we suppressed the ω dependence of these functions. G_0 in Eq. (14) precisely corresponds to the Green's function defined in the harmonic case in Sec. III. The second equation in (14) is known as the ‘‘Keldysh equation’’ [109]. In the absence of anharmonic interaction, $\Sigma_n = 0$, the Meir-Wingreen expression reduces to the Landauer formula with the transmission function Eq. (5). In the interacting case it can be organized and expressed in terms of an effective, temperature-dependent, transmission function [26, 113],

$$\begin{aligned} \mathcal{T}_{\text{eff}}(\omega, T_L, T_R) &\equiv \text{Tr}[G^r \Gamma_L G^a \Gamma_R] \\ &+ \frac{1}{2(n_L - n_R)} \text{Tr}[G^r \Gamma_n G^a (n_L \Gamma_L - n_R \Gamma_R) - iG^r \Sigma_n^< G^a (\Gamma_L - \Gamma_R)], \end{aligned} \quad (15)$$

where $\Gamma_n = i(\Sigma_n^r - \Sigma_n^a)$ and n_ν denotes the Bose-Einstein distribution function of the ν bath. Under a symmetric coupling, $\Gamma_L = \Gamma_R = \Gamma$, the transmission function reduces to

$$\mathcal{T}_{\text{eff}}^{\text{sym}}(\omega, T_L, T_R) = \frac{1}{2} \text{Tr}[A(\omega)\Gamma(\omega)], \quad (16)$$

with $A(\omega) \equiv i[G^r(\omega) - G^a(\omega)]$ as the spectral function of the molecule.

The Meir-Wingreen formula (13) is formally exact, but approximations should be employed to compute the nonlinear self-energy, hence the current. Computational treatments include the standard quantum field theory-type perturbative scheme using the Feynman diagrammatic approach [113–115], and self-consistent approaches [26, 28, 116–119] in which the harmonic Green's function G_0 in Σ_n is replaced by the full nonlinear G . In fact, the self-consistent approach under certain conditions provides results in agreement with quantum master equation treatments [120, 121], when the molecule-reservoir coupling is sufficiently weak.

What is the physical content of the retarded nonlinear self-energy Σ_n^r ? Its real part is responsible for frequency shifts of molecular vibrational modes. The imaginary part corresponds to the finite life-time of phonons, eventually responsible for the development of diffusive dynamics. It should be mentioned though that to fully realize the diffusive regime, high order phonon scattering processes should be included in the nonlinear self-energy. Once extracting the phonon lifetime τ_q , the thermal conductivity (denoted here by $\tilde{\kappa}$) can be computed from the Boltzmann transport equation or more simply, using the standard kinetic theory formula $\tilde{\kappa} = \sum_q \frac{1}{3} c_q v_q^2 \tau_q$, where c_q is the heat capacity per unit volume of mode q and v_q is the phonon group velocity [122].

2. Application

The Landauer formula (4) was derived under the harmonic approximation thus it rules out thermal rectification effects and other nontrivial nonlinear functionalities [13]. The NEGF formalism, in contrast, allows us to evaluate the role of anharmonicities in energy transport. We exemplify the utility of the method on the single atom junction [recall Eq. (11)], allowing the oscillator to further interact with a quartic pinning potential with the Hamiltonian $H_n = \frac{\epsilon}{4} u_0^4$ [123]. To the lowest (first) order in ϵ , the components of the nonlinear self-energy are given by $\Sigma_n^r(\omega) = \Sigma_n^a(\omega) = 3i\hbar\epsilon G_0^<(t=0)$, $\Sigma_n^<(\omega) = \Sigma_n^>(\omega) = 0$. Using these terms in Eq. (15), the transmission function with nonlinearities $\mathcal{T}_n(\omega)$ can be expressed in terms of the harmonic result $\mathcal{T}(\omega)$ [124],

$$\begin{aligned} \mathcal{T}_n(\omega; T_L, T_R) &= (1 + \Lambda(\omega; T_L, T_R)) \mathcal{T}(\omega), \\ \Lambda(\omega; T_L, T_R) &= 6i\hbar\epsilon G_0^<(t=0) \text{Re}[G_0^r(\omega)]. \end{aligned} \quad (17)$$

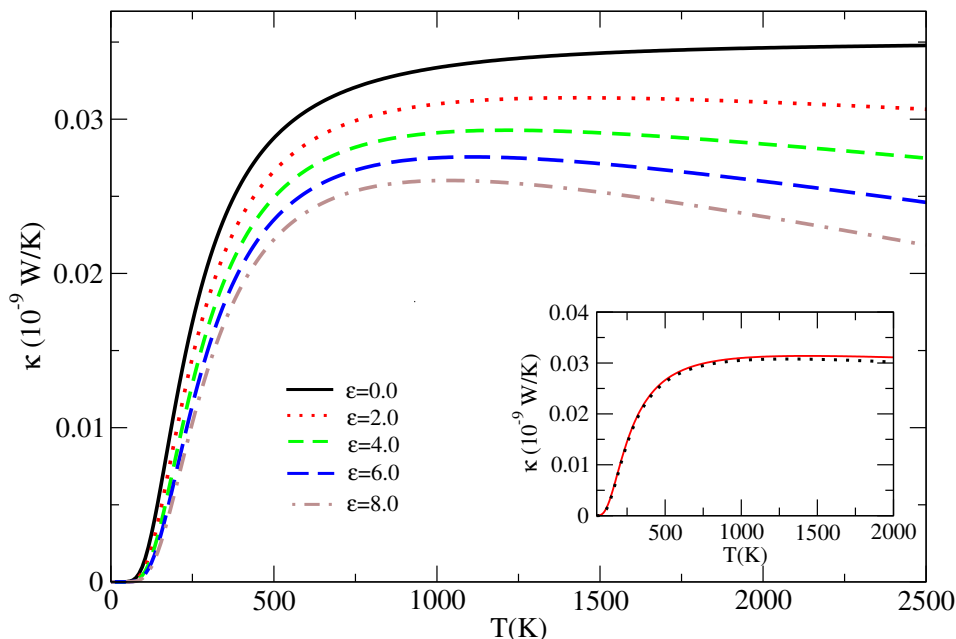


FIG. 6: Self-consistent NEGF calculations of the thermal conductance as a function of temperature T for an anharmonic junction. The single harmonic oscillator junction ($\epsilon = 0$) is supplemented by a quartic onsite potential $H_n = \frac{\epsilon}{4}u_0^4$. ϵ is given in units of $\text{eV}/(\text{amu}^2\text{\AA}^4)$. The reservoirs are defined by semi-infinite chains of harmonic oscillators with the nearest-neighbors force constant $k = 1 \text{ eV}/(\text{amu}\text{\AA}^2)$ and an onsite element $k_0 = 0.1k$. The “molecule” includes a single oscillator with $K_S = 1.1k$, and it is coupled to the left and right solids through $\Lambda_{-1,0}^{LS} = \Lambda_{0,1}^{SR} = -0.25k$. The inset compares the thermal conductance as calculated using the self-consistent procedure (solid line) and the first-order expression (17) (dotted line) for $\epsilon = 2 \text{ eV}/(\text{amu}^2\text{\AA}^4)$. Adapted with permission from [123].

It should be recognized that the lesser component of the Green’s function, $G_0^<(t=0)$, depends on temperature. As a result, the effective transmission function becomes temperature dependent and the junction can manifest nonlinear functionalities such as the diode effect.

Fig. (6) displays the thermal conductance of this single anharmonic oscillator junction, plotted against the averaged temperature T . Simulations were performed by employing the self-consistent NEGF approach, replacing G_0 by the full G in Σ_n , and solving the Keldysh equation (14) iteratively, to compute the current from Eq. (13) [123]. It is evident that at low temperatures the junction’s thermal conductance is dominated by elastic-harmonic forces. In contrast, at high temperatures the thermal conductance is significantly reduced when the anharmonic pinning potential is turned on, as inelastic phonon scattering processes largely influence transport.

The NEGF technique as described here is limited to small-atomistic models. Efforts are dedicated to link and interface NEGF results with coarse-gained modeling such as the Boltzmann transport equation. This would allow simulations of larger nanoscale systems, and the resolution of e.g. ballistic-diffusive crossover with parameter-free quantum mechanical first principle approaches [122].

C. Quantum Master Equation

Projection Operator approaches, such as the Nakajima-Zwanzig projection operator technique [125], trace out the dynamics of the (non-interesting) bath degrees of freedom, to reach equations of motion for relevant-subsystem coordinates, typically, under the assumption of fast dynamics for the bath relative to the subsystem. At the heart of such approaches is the conceptual separation of the model into three constituents: subsystem of interest, environment, and an interaction term between the components. Quantum master equations (QME) which describe the reduced dynamics of the density operator are immensely useful for modelling electron, proton, and exciton transfer, vibrational relaxation and spin dynamics in condensed phases [126]. As well, in the related optical QME the radiation field plays the role of a thermal environment [125]. Standard approximations involved in the framework of QME are: (i) weak subsystem-bath coupling, allowing a perturbative expansion in the interaction strength. (ii) Markov approximation,

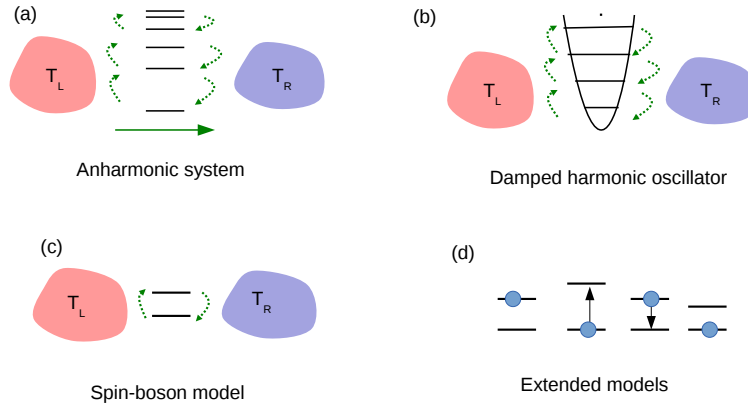


FIG. 7: Thermal nanojunctions in the energy representation for the molecular subsystem. (a) Generic anharmonic junction. (b) Damped harmonic oscillator model, generalized to the non-equilibrium case. (c) Spin-boson model with an anharmonic, two-level system, coupled to harmonic baths. (d) An extended-site model which can describe e.g. spin and exciton transfer in chains. The arrows describe an energy transfer process, with a certain site being excited simultaneously with the de-excitation of a different site

assuming short-lived memory effects in the bath, and (iii) rotating wave approximation (often employed in the quantum optics literature), leaving out off-resonant terms.

QME traditionally communicate the dynamics, population and coherences, of a subsystem of interest. More recently, efforts were put forward for the development of related schemes for transport coefficients, to calculate (charge, heat, spin) currents in non-equilibrium situations. Advantages of QME over other approaches such as the NEGF are: (i) It can treat exactly intrinsic anharmonicities, yet obviously, limited to small “impurity” models. (ii) Analytic results can be derived, to expose the role of different factors in the heat transport behavior. The QME approach can be conveniently formulated in the energy basis of the subsystem. Some examples in the context of vibrational heat flow in molecular junctions are illustrated in Fig. 7.

1. Weak molecule-reservoir coupling: The Bloch-Redfield-Markov equation

We bring here a brief description of QME for vibrational heat transport in junctions, under the assumption of weak molecule-bath coupling, by following Refs. [63, 92]. Fig. 7(a) displays the model, an N -state subsystem (possibly many-body nonlocal states) and two heat baths. Excitation and relaxation processes in the subsystem are induced by complementing processes in the reservoirs. The total Hamiltonian is

$$H = H_S + H_L + H_R + V_L + V_R, \quad (18)$$

where

$$H_S = \sum_n E_n |n\rangle\langle n|, \quad V_\nu = S^\nu \otimes B^\nu, \quad \nu = L, R. \quad (19)$$

The energy spectrum of the subsystem (molecule) E_n may be derived from a truly anharmonic potential without further approximations. In the damped harmonic oscillator model of Fig. 7(b), $E_n = n\hbar\omega_0$. The molecular system is coupled to thermal baths H_ν , $\nu = L, R$, not necessarily harmonic [see examples in Refs. [64, 92]], with the subsystem operators $S^\nu = \sum_{m,n} S_{m,n}^\nu |m\rangle\langle n|$ and the operator B^ν , given in terms of the ν bath degrees of freedom. Leaving out details, it can be shown that the population P_n of the subsystem eigenstates obey kinetic equations [92]

$$\dot{P}_n(t) = -P_n(t) \sum_{\nu,m} |S_{n,m}^\nu|^2 k_{n \rightarrow m}^\nu + \sum_{\nu,m} |S_{n,m}^\nu|^2 k_{m \rightarrow n}^\nu P_m(t), \quad (20)$$

with rate constants

$$k_{n \rightarrow m}^\nu = \int_{-\infty}^{\infty} e^{-iE_{n,m}\tau/\hbar} \langle B_\nu(\tau) B_\nu(0) \rangle_{T_\nu} d\tau. \quad (21)$$

This result is correct to the lowest nontrivial order in the subsystem-bath coupling. It was derived under a Markovian approximation, and after decoupling the diagonal and off-diagonal elements of the reduced density matrix. The operators in Eq. (21) are given in the interaction representation, $\langle \dots \rangle_T$ represents an average with respect to the equilibrium distribution of the two baths, $E_{m,n} \equiv E_m - E_n$. Applying similar steps, the steady state heat current across the system [depicted in Fig. 7(a)] explicitly follows [63, 92]

$$j_q = \frac{1}{2} \sum_{n>m} E_{m,n} |S_{m,n}^L|^2 [P_n k_{n \rightarrow m}^L - P_m k_{m \rightarrow n}^L] - \frac{1}{2} \sum_{n>m} E_{m,n} |S_{m,n}^R|^2 [P_n k_{n \rightarrow m}^R - P_m k_{m \rightarrow n}^R]. \quad (22)$$

Here, the population P_n are the long-time solution of Eq. (20). This symmetric expression is quite intuitive: The current is given by calculating the net transfer process from all transitions between the n and m states. Rate constants are multiplied by energy differences and weighted by the population of states. A more general result, involving contributions from coherences, was derived in Ref. [45].

We exemplify this expression in the “atomic limit”, with a junction comprising of a single oscillator. In the harmonic limit, using the bosonic creation $b_{\nu,q}^\dagger$ and annihilation $b_{\nu,q}$ operators, $H_\nu = \sum \hbar\omega_q b_{\nu,q}^\dagger b_{\nu,q}$, $H_S = \hbar\omega_0 b_0^\dagger b_0$, $V_\nu = \sum_{\nu,q} \frac{\hbar\tilde{\lambda}_{\nu,q}}{2} (b_{\nu,q}^\dagger + b_{\nu,q})(b_0^\dagger + b_0)$, one can derive the Landauer-like result,

$$j_q = \hbar\omega_0 \frac{\gamma_L(\omega_0)\gamma_R(\omega_0)}{\gamma_L(\omega_0) + \gamma_R(\omega_0)} [n_L(\omega_0) - n_R(\omega_0)], \quad (23)$$

where $\gamma_\nu(\omega) = \pi/2 \sum_q \tilde{\lambda}_{\nu,q}^2 \delta(\omega - \omega_q)$ stands for the mode-bath coupling energy, consistent with the definitions of the damping function in Sec. III A. Eq. (23) can be obtained from Eq. (12) taking the limit $\gamma_\nu \ll \omega_0$, and it describes a resonant-sequential transmission process, as only reservoirs’ modes which match the molecular frequency ω_0 scatter through the junction.

Beyond the harmonic approximation, the “spin boson model” is a simple yet truly nontrivial example for anharmonic heat conduction. In this case, the subsystem spectrum is truncated to include only two states with a gap ω_0 , see Fig. 7(c). The spin-boson Hamiltonian includes a two-state “impurity”, $H_S = \frac{\hbar\omega_0}{2} \sigma_z$, interacting with harmonic baths $H_\nu = \sum \hbar\omega_q b_{\nu,q}^\dagger b_{\nu,q}$ according to $V_\nu = \sigma_x \sum_q \frac{\hbar\tilde{\lambda}_{\nu,q}}{2} (b_{\nu,q}^\dagger + b_{\nu,q})$. Here σ_x and σ_z are the Pauli matrices. Using Eqs. (20)-(22), one receives now the heat current [46, 63]

$$j_q = \hbar\omega_0 \frac{\gamma_L(\omega_0)\gamma_R(\omega_0)}{\gamma_L(\omega_0)[1 + 2n_L(\omega_0)] + \gamma_R(\omega_0)[1 + 2n_R(\omega_0)]} [n_L(\omega_0) - n_R(\omega_0)]. \quad (24)$$

Since the baths temperatures enter the transmission probability here, this junction can display the thermal diode effect when spatial asymmetries are presented [46]. This nonlinear functionality is a definite fingerprint of anharmonic terms.

The weak-coupling second order QME presented here can be extended systematically to higher orders, to account e.g. for co-tunneling processes [127]. Insight can be also earned by writing down Fermi-golden rule rates for multi-phonon scattering processes, then constructing the overall heat transfer rate, or the thermal current, based on the framework of kinetic master equations [8, 128, 129]. For a cubic anharmonicity, for example, Fermi golden rule rates consist two types of (energy conserving) processes: a vibrational mode may decay into two others, or two modes can collide to produce a third mode. This type of analysis is particularly useful for simulating vibrational energy transfer in amorphous materials, glasses [130], proteins [129, 131–133] and across interfaces [48].

2. Strong molecule-surface coupling: polaronic equations

Equation (22) was derived under the assumption of a molecule weakly attached to the thermal reservoirs. It predicts a linear enhancement of the thermal conductance with increasing coupling energy γ , see for example Eq. (23). Obviously, at strong coupling, corresponding to a molecule tightly attached to the interface, this trend should break down. By using the so-called non-interacting-blip approximation (NIBA) [134], which is related to a polaronic treatment [135], it was recently demonstrated that the thermal conductance of the anharmonic spin-boson model (with an ohmic dissipation) displays a crossover behavior with the system-bath coupling parameter, satisfying $\kappa \propto \frac{k_B\omega_0^2}{\omega_c} \left(\frac{\hbar\omega_c}{k_B T} \right)^{1-2\alpha}$; $\alpha = \alpha_L + \alpha_R$ [136]. We used the ohmic damping function, $\gamma_\nu(\omega) = \pi\alpha_\nu\omega e^{-\omega/\omega_c}$ with ω_c the Debye (cutoff) frequency of the phononic baths and α a dimensionless parameter. It is also useful to define $E_r \equiv 2\alpha_\nu\omega_c$ as the reorganization-interaction energy of the molecular mode with the baths’ phonons. This NIBA result for the conductance agrees with numerically exact Monte-Carlo simulations, at high temperatures [97].

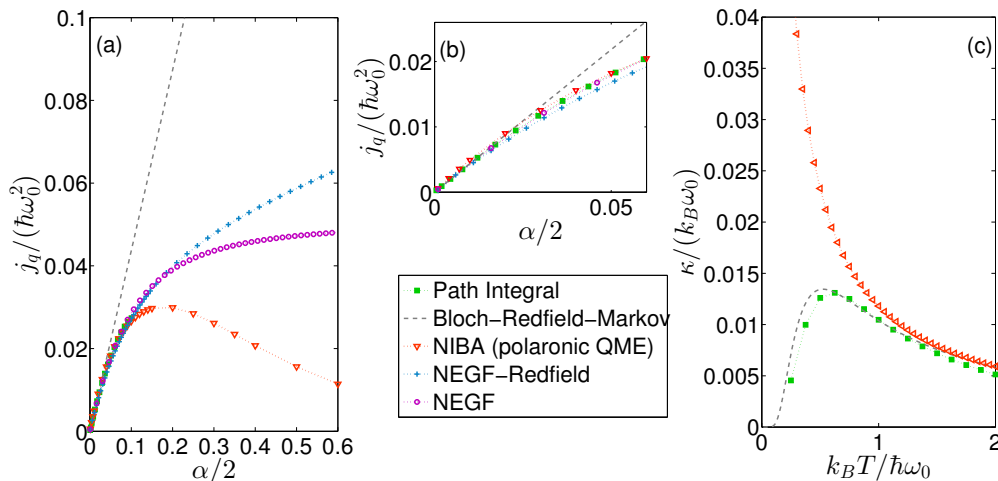


FIG. 8: Heat transfer in an anharmonic nanojunction, the spin-boson model of Fig. 7(c). (a) Current as a function of the molecule-bath coupling parameter $\alpha = \alpha_L + \alpha_R$, demonstrating the breakdown of the linear scaling predicted by the weak coupling Bloch-Redfield-Markov QME [98], with a suppression of the current at strong coupling. Panel (b) Zooms over the weak coupling regime where different approximations agree. $k_B T_L = 2\omega_0$ and $k_B T_R = \omega_0$, $\omega_c/\omega_0 = 10$. (c) Thermal conductance $\kappa = j_q/\Delta T$ as a function of temperature in the linear response regime, $\Delta T = T_L - T_R$. NIBA (polaronic QME) correctly behaves only at high temperatures. $\omega_c/\omega_0 = 10$ and $\alpha_{L,R} = 0.0172$. For more details, see Ref. [98].

Fig. 8 displays the heat current in the spin-boson model, a representative of an anharmonic junction, under different approximation schemes: a standard weak-coupling treatment (Bloch-Redfield-Markov QME), NIBA-polaronic QME, an NEGF-Redfield approach [112] and a more accurate variant of NEGF [137], as well as numerically-exact influence functional path integral simulations [138], performed based on the mapping of the model onto a fermionic description. For more details, see Ref. [98]. We make the following observations: (i) The trend $j_q \propto \alpha$ fails beyond the very-weak coupling limit. (ii) At high temperatures, $k_B T > \hbar\omega_0$, the thermal conductance decays with the increase of temperature, a manifestation of the intrinsic anharmonicity of the junction. This trend is correctly captured by QME calculations, see Fig. 8(c). In contrast, at low temperatures this trend is reversed since thermal occupation factors of bath modes dominate the behavior, rather than temperature-dependent (anharmonic) effects on the junction. NIBA simulations, however, fail to capture this turnover behavior. Approximate techniques which can bridge between different regimes, to consistently describe transport e.g. at weak and strong coupling, are of great interest [139], as well as the derivation of bounds for heat transport in anharmonic junctions [140].

D. Numerically-Exact Simulations

The methods detailed so far are limited to describe heat conduction in certain physical regimes due to their underlying approximations, as exemplified in Fig. 8. It is highly desirable thus to develop first-principle techniques which can go beyond perturbation theories, to reveal the crossover between different regimes and to provide benchmarks for approximate theories. Obviously, such nonperturbative treatments are numerical in nature and computationally limited to the simulation of minimal nanojunctions such as the two-bath spin-boson model. The dissipative dynamics of a two-state system coupled to a single heat bath, the (original) spin-boson model, has been examined in many studies [141]. Among the numerically exact machinery employed to treat it we list the quasi-adiabatic propagator path-integral (QUAPI) approach [142, 143], which builds upon the Feynman-Vernon influence functional, the multiconfiguration time-dependent Hartree (MCTDH) method, a wavefunction theory [144], and Monte Carlo (MC) simulations [145]. These tools were developed to hand over the dynamics of the reduced density matrix of the subsystem. However, a current operator is a more complex object in nature since it is explicitly defined in terms of the baths degrees of freedom.

Generalizations of numerically exact tools to simulate phononic heat current were reported in several recent studies: The multilayer multiconfiguration time-dependent Hartree theory was extended in Ref. [96], and it revealed a turnover behavior of the current with increasing coupling strength, similarly to Fig. 8(a). Influence-functional path integral

simulations were employed in Refs. [98, 146], by mapping boson environments into fermion baths [138]. Monte Carlo simulations of the (linear response) thermal conductance were performed in [97], by mapping the spin-boson model onto an Ising model with long-range exchange interactions. More recently, influence function path integral expressions were generalized to describe heat exchange between a subsystem and a heat bath [147], though a calculation of the steady state heat current under a QUAPI-type approach is still missing.

These numerically exact treatments are limited to a minimal anharmonic heat conducting nanojunction, a qubit, yet they are immensely useful for our understanding of quantum transport in hybrid junctions [18] in a broad range of parameters: under weak/strong coupling of the subsystem to the heat baths, low/high temperatures, slow/fast subsystem dynamics relative to the baths' motion, and when different baths are employed, e.g., with rich spectral properties, possibly taking into account bath anharmonicities. Future studies will aim to bridge the gap between minimal models and more physical realizations of anharmonic junctions.

V. CONCLUSIONS

In this review, we focused on the problem of vibrational energy transfer (or thermal/heat/phononic conduction) in a junction geometry with a molecule bridging two heat reservoirs. We described recent experiments on vibrational heat transfer in molecular junctions focusing on alkane chains. We then reviewed methodologies useful for calculating thermal conduction in the quantum domain, starting from coherent-harmonic phononic conduction in nanojunctions, and concluding with highly-anharmonic yet minimal qubit constructions. We began by recounting the Landauer approach, appropriate for the study of elastic transport. This simple tool can be readily employed to simulate phononic conduction in extended systems, as long as the molecular normal modes and their hybridization with the contacts are given. The Landauer-elastic scattering picture breaks down when interactions (anharmonicities) are presented. We outlined several techniques which account for anharmonic effects: The self-consistent reservoirs method mimics inelastic scattering of phonons with temperature probes. The non-equilibrium Green's function technique as described here accounts for genuine many-body effects, albeit perturbatively, and it is limited to simple-minimal models. Reduced density matrix projection operator techniques can be extended to study thermal conduction of "impurity models", when a molecule is strongly coupled to macroscopic solids. Finally, numerically exact techniques can simulate heat exchange in minimal models such as the spin-boson nanojunction, providing benchmarks for approximate techniques.

Developing techniques for computing quantum heat transfer in nanostructures, bridging the gap between minimal-model junctions and real systems, is highly desirable. Ongoing efforts are dedicated towards the development of semiclassical techniques in which quantum statistics is implemented within classical molecular dynamics simulations [148, 149], construction of quantum corrections to classical expressions [25, 150], and computations using Boltzmann transport equation with input from first-principle atomistic approaches [122].

In this review we only considered conduction of heat due to vibrations of nuclear degrees of freedom. However, when a molecule links metal electrodes, electrons as well considerably participate in the heat conduction process. Understanding how the interaction between electrons and atomic vibrations affect electron dynamics as well as energy transfer in real systems is a fundamental-formidable task, groundwork for making further progress in molecular nanotechnology.

ACKNOWLEDGMENTS

This work was funded by the Natural Sciences and Engineering Research Council of Canada, the Canada Research Chair Program and the CQIQC at the University of Toronto. We thank Renante Yson for assistance in generating graphics.

-
- [1] Pop E. 2010. Energy dissipation and transport in nanoscale devices. *Nano Res.* 3:147
 - [2] Moore AL, Shi L. 2014. Emerging challenges and materials for thermal management of electronics. *Materials Today* 17:163–174
 - [3] Balandin AA. 2011. Thermal properties of graphene and nanostructured carbon materials. *Nature Materials* 10:569–581
 - [4] Dresselhaus M, Chen G, Tang M, Yang R, Lee H, et al. 2007. New directions for low-dimensional thermoelectric materials. *Adv. Mater.* 19:1043–1053
 - [5] Shakouri A. 2011. In *Ann. Rev. Mater. Res.*, ed. Clarke, DR and Fratzl, P, vol. 41. 399–431
 - [6] Flynn GW, Parmenter CS, Wodtke AM. 1996. Vibrational energy transfer. *J. Phys. Chem.* 100:12817–12838
 - [7] Gruebele M, Wolynes PG. 2004. Vibrational energy flow and chemical reactions. *Acc. Chem. Res.* 37:261–267

- [8] Leitner D. 2008. Energy flow in proteins. *Ann. Rev. Phys. Chem.* 59:233–259
- [9] Cahill DG, Braun PV, Chen G, Clarke DR, Fan S, et al. 2014. Nanoscale thermal transport. ii. 2003–2012. *App. Phys. Rev.* 1:011305
- [10] Schwarzer D, Kutne P, Schröder C, Troe J. 2004. Intramolecular vibrational energy redistribution in bridged azulene-anthracene compounds: Ballistic energy transport through molecular chains. *J. Chem. Phys.* 121:1754–1764
- [11] Bergfield JP, Ratner MA. 2013. Forty years of molecular electronics: Non-equilibrium heat and charge transport at the nanoscale. *Phys. Status Solidi (b)* 250:2249–2266
- [12] Aradhyia SV, Venkataraman L. 2013. Single-molecule junctions beyond electronic transport. *Nature Nanotech.* 8:399–410
- [13] Li N, Ren J, Wang L, Zhang G, Hänggi P, Li B. 2012. Colloquium: Phononics: Manipulating heat flow with electronic analogs and beyond. *Rev. Mod. Phys.* 84:1045
- [14] Yang N, Xu X, Zhang G, Li B. 2012. Thermal transport in nanostructures. *AIP Advances* 2:041410
- [15] Bauer GEW, Saitoh E, van Wees BJ. 2012. Spin caloritronics. *Nature Materials* 11:391–399
- [16] Ekinici K, Roukes M. 2005. Nanoelectromechanical systems. *Rev. Sci. Instr.* 76
- [17] Aspelmeier M, Kippenberg TJ, Marquard F. 2014. Cavity optomechanics. *Rev. Mod. Phys.* 86:1391–1452
- [18] Xiang ZL, Ashhab S, You J, Nori F. 2013. Hybrid quantum circuits: Superconducting circuits interacting with other quantum systems. *Rev. Mod. Phys.* 85:623
- [19] Dhar A. 2008. Heat transport in low-dimensional systems. *Adv. Phys.* 57:457
- [20] Terraneo M, Peyrard M, Casati G. 2002. Controlling the energy flow in nonlinear lattices: A model for a thermal rectifier. *Phys. Rev. Lett.* 88:094302
- [21] Luo T, Chen G. 2013. Nanoscale heat transfer - from computation to experiment. *Phys. Chem. Chem. Phys.* 15:3389–3412
- [22] Marconnet AM, Panzer MA, Goodson KE. 2013. Thermal conduction phenomena in carbon nanotubes and related nanostructured materials. *Rev. Mod. Phys.* 85:1295–1326
- [23] Dubi Y, Di Ventra M. 2011. Colloquium: Heat flow and thermoelectricity in atomic and molecular junctions. *Rev. Mod. Phys.* 83:131
- [24] Lepri S, Livi R, Politi A. 2003. Thermal conduction in classical low-dimensional lattices. *Phys. Rep.* 377:1–80
- [25] McGaughey A, Kaviany M. 2006. vol. 39 of *Adv. Heat Trans.* Elsevier, 169–255
- [26] Wang JS, Wang J, Lu JT. 2008. Quantum thermal transport in nanostructures. *Euro. Phys. J. B* 62:381–404
- [27] Wang JS, Agarwalla BK, Li H, Thingna J. 2014. Nonequilibrium greens function method for quantum thermal transport. *Front. Phys.* 9:673–697
- [28] Mingo N. 2009. In *Thermal nanosystems and nanomaterials*. Springer Berlin Heidelberg, 63–94
- [29] Galperin M, Ratner MA, Nitzan A. 2007. Molecular transport junctions: vibrational effects. *J. Phys.: Condensed Matter* 19:103201
- [30] Galperin M, Nitzan A, Ratner MA. 2007. Heat conduction in molecular transport junctions. *Phys. Rev. B* 75:155312
- [31] Wang RY, Segalman RA, Majumdar A. 2006. Room temperature thermal conductance of alkanedithiol self-assembled monolayers. *App. Phys. Lett.* 89:173113
- [32] Meier T, Menges F, Nirmalraj P, Hölscher H, Riel H, Gotsmann B. 2014. Length-dependent thermal transport along molecular chains. *Phys. Rev. Lett.* 113:060801
- [33] Losego MD, Grady ME, Sottos NR, Cahill DG, Braun PV. 2012. Effects of chemical bonding on heat transport across interfaces. *Nature Materials* 11:502–506
- [34] Carter JA, Wang Z, Dlott DD. 2009. Ultrafast nonlinear coherent vibrational sum-frequency spectroscopy methods to study thermal conductance of molecules at interfaces. *Acc. Chem. Res.* 42:1343–1351
- [35] Rubtsova NI, Nyby CM, Zhang H, Zhang B, Zhou X, et al. 2015. Room-temperature ballistic energy transport in molecules with repeating units. *J. Chem. Phys.* 142:212412
- [36] Rubtsova NI, Rubtsov IV. 2015. In *Annu. Rev. Phys. Chem.*, ed. Johnson, MA and Martinez, TJ, vol. 66 of *Annu. Rev. Phys. Chem.* . 717–738
- [37] Botan V, Backus EH, Pfister R, Moretto A, Crisma M, et al. 2007. Energy transport in peptide helices. *Proc. Natl. Acad. Sci. USA* 104:12749–12754
- [38] Segal D, Nitzan A, Hänggi P. 2003. Thermal conductance through molecular wires. *J. Chem. Phys.* 119:6840–6855
- [39] Majumdar S, Sierra-Suarez JA, Schiffres SN, Ong WL, Higgs CF, et al. 2015. Vibrational mismatch of metal leads controls thermal conductance of self-assembled monolayer junctions. *Nano Lett.* 15:2985–2991
- [40] Wang Z, Carter JA, Lagutchev A, Koh YK, Seong NH, et al. 2007. Ultrafast flash thermal conductance of molecular chains. *Science* 317:787–790
- [41] Wang Z, Cahill DG, Carter JA, Koh YK, Lagutchev A, et al. 2008. Ultrafast dynamics of heat flow across molecules. *Chem. Phys.* 350:31–44. Femtochemistry and Femtobiology Papers associated with the 8th International Conference on Femtochemistry and Femtobiology
- [42] Yue Y, Qasim LN, Kurnosov AA, Rubtsova NI, Mackin RT, et al. 2015. Band-selective ballistic energy transport in alkane oligomers: Toward controlling the transport speed. *J. Phys. Chem. B* 119:6448–6456
- [43] Kim P, Shi L, Majumdar A, McEuen PL. 2001. Thermal transport measurements of individual multiwalled nanotubes. *Phys. Rev. Lett.* 87:215502
- [44] Schade M, Hamm P. 2012. Transition from IVR-limited vibrational energy transport to bulk heat transport. *Chem. Phys.* 393:46–50
- [45] Thingna J, García-Palacios J, Wang JS. 2012. Steady-state thermal transport in anharmonic systems: Application to molecular junctions. *Phys. Rev. B* 85:195452
- [46] Segal D, Nitzan A. 2005. Spin-boson thermal rectifier. *Phys. Rev. Lett.* 94:034301

- [47] Wu LA, Segal D. 2009. Sufficient conditions for thermal rectification in hybrid quantum structures. *Phys. Rev. Lett.* 102:095503
- [48] Leitner DM. 2013. Thermal boundary conductance and thermal rectification in molecules. *J. Phys. Chem. B* 117:12820–12828
- [49] Pein BC, Sun Y, Dlott DD. 2013. Unidirectional vibrational energy flow in nitrobenzene. *J. Phys. Chem. A* 117:6066–6072
- [50] Pein BC, Dlott DD. 2014. Modifying vibrational energy flow in aromatic molecules: Effects of ortho substitution. *J. Phys. Chem. A* 118:965–973
- [51] Pein BC, Sun Y, Dlott DD. 2013. Controlling vibrational energy flow in liquid alkylbenzenes. *J. Phys. Chem. B* 117:10898–10904
- [52] Zürcher U, Talkner P. 1990. Quantum-mechanical harmonic chain attached to heat baths. ii. nonequilibrium properties. *Phys. Rev. A* 42:3278–3290
- [53] Dhar A, Roy D. 2006. Heat transport in harmonic lattices. *J. Stat. Phys.* 125:801–820
- [54] Panasyuk GY, Levin GA, Yerkes KL. 2012. Heat exchange mediated by a quantum system. *Phys. Rev. E* 86:021116
- [55] Ozpineci A, Ciraci S. 2001. Quantum effects of thermal conductance through atomic chains. *Phys. Rev. B* 63:125415
- [56] Patton KR, Geller MR. 2001. Thermal transport through a mesoscopic weak link. *Phys. Rev. B* 64:155320
- [57] Landauer R. 1957. Spatial variation of currents and fields due to localized scatterers in metallic conduction. *IBM J. Res. Dev.* 1:223–231
- [58] Saito K, Dhar A. 2007. Fluctuation theorem in quantum heat conduction. *Phys. Rev. Lett.* 99:180601
- [59] Agarwalla BK, Li B, Wang JS. 2012. Full-counting statistics of heat transport in harmonic junctions: Transient, steady states, and fluctuation theorems. *Phys. Rev. E* 85:051142
- [60] Rego LGC, Kirczenow G. 1998. Quantized thermal conductance of dielectric quantum wires. *Phys. Rev. Lett.* 81:232–235
- [61] Caroli C, Combescot R, Nozieres P, Saint-James D. 1971. *J. Phys. C: Solid St. Phys.* 4:916
- [62] Walczak K, Yerkes KL. 2014. Nanoscale transport of phonons: Dimensionality, subdiffusion, molecular damping, and interference effects. *J. App. Phys.* 115:174308
- [63] Segal D. 2006. Heat flow in nonlinear molecular junctions: Master equation analysis. *Phys. Rev. B* 73:205415
- [64] Segal D. 2008. Single mode heat rectifier: Controlling energy flow between electronic conductors. *Phys. Rev. Lett.* 100:105901
- [65] Vinkler-Aviv Y, Schiller A, Andrei N. 2014. Single-molecule-mediated heat current between an electronic and a bosonic bath. *Phys. Rev. B* 89:024307
- [66] Pendry JB. 1983. Quantum limits to the flow of information and entropy. *J. Phys. A: Math. Gen.* 16:2161
- [67] Käso M, Wulf U. 2014. Quantized thermal conductance via phononic heat transport in nanoscale devices at low temperatures. *Phys. Rev. B* 89:134309
- [68] Schwab K, Henriksen EA, Worlock JM, Roukes ML. 2000. Measurement of the quantum of thermal conductance. *Nature* 404:974–977
- [69] McConnell HM. 1961. Intramolecular charge transfer in aromatic free radicals. *J. Chem. Phys.* 35:508–515
- [70] Markussen T. 2013. Phonon interference effects in molecular junctions. *J. Chem. Phys.* 139:244101
- [71] Mingo N, Broido DA. 2005. Carbon nanotube ballistic thermal conductance and its limits. *Phys. Rev. Lett.* 95:096105
- [72] Yamamoto T, Watanabe K. 2006. Nonequilibrium green’s function approach to phonon transport in defective carbon nanotubes. *Phys. Rev. Lett.* 96:255503
- [73] Kiršanskas G, Li Q, Flensburg K, Solomon GC, Leijnse M. 2014. Designing π -stacked molecular structures to control heat transport through molecular junctions. *App. Phys. Lett.* 105:233102
- [74] Arroyo CR, Tarkuc S, Frisenda R, Seldenthuis JS, Woerde CHM, et al. 2013. Signatures of quantum interference effects on charge transport through a single benzene ring. *Angew. Chem.* 125:3234–3237
- [75] Manrique DZ, Huang C, Baghernejad M, Zhao X, Al-Owaedi OA, et al. 2015. A quantum circuit rule for interference effects in single-molecule electrical junctions. *Nature Comm.* 6
- [76] Fermi E, Pasta J, Ulam S. 1965. *Collected Papers of Enrico Fermi, edited by E. Segre* :978–988
- [77] Schelling PK, Phillpot SR, Keblinski P. 2002. Comparison of atomic-level simulation methods for computing thermal conductivity. *Phys. Rev. B* 65:144306
- [78] He Y, Savic I, Donadio D, Galli G. 2012. Lattice thermal conductivity of semiconducting bulk materials: atomistic simulations. *Phys. Chem. Chem. Phys.* 14:16209–16222
- [79] Chaudhuri A, Kundu A, Roy D, Dhar A, Lebowitz JL, Spohn H. 2010. Heat transport and phonon localization in mass-disordered harmonic crystals. *Phys. Rev. B* 81:064301
- [80] Dhar A. 2001. Heat conduction in the disordered harmonic chain revisited. *Phys. Rev. Lett.* 86:5882–5885
- [81] Lee LW, Dhar A. 2005. Heat conduction in a two-dimensional harmonic crystal with disorder. *Phys. Rev. Lett.* 95:094302
- [82] Lepri S, Livi R, Politi A. 1997. Heat conduction in chains of nonlinear oscillators. *Phys. Rev. Lett.* 78:1896–1899
- [83] Dhar A, Saito K. 2008. Heat conduction in the disordered fermi-pasta-ulam chain. *Phys. Rev. E* 78:061136
- [84] Saito K, Dhar A. 2010. Heat conduction in a three dimensional anharmonic crystal. *Phys. Rev. Lett.* 104:040601
- [85] Das SG, Dhar A, Narayan O. 2014. Heat conduction in the fermipastaulam chain. *J. Stat. Phys.* 154:204–213
- [86] Liu S, Agarwalla BK, Wang JS, Li B. 2013. Classical heat transport in anharmonic molecular junctions: Exact solutions. *Phys. Rev. E* 87:022122
- [87] Li B, Wang L, Casati G. 2006. Negative differential thermal resistance and thermal transistor. *App. Phys. Lett.* 88:143501
- [88] Li B, Wang L, Casati G. 2004. Thermal diode: Rectification of heat flux. *Phys. Rev. Lett.* 93:184301
- [89] Yang N, Zhang G, Li B. 2008. Carbon nanocone: A promising thermal rectifier. *App. Phys. Lett.* 93:243111
- [90] Lo WC, Wang L, Li B. 2008. Thermal transistor: Heat flux switching and modulating. *J. Phys. Soc. Japan* 77:054402

- [91] Wang L, Li B. 2008. Thermal memory: A storage of phononic information. *Phys. Rev. Lett.* 101:267203
- [92] Wu LA, Yu CX, Segal D. 2009. Nonlinear quantum heat transfer in hybrid structures: Sufficient conditions for thermal rectification. *Phys. Rev. E* 80:041103
- [93] Wu LA, Segal D. 2011. Quantum heat transfer: A born-oppenheimer method. *Phys. Rev. E* 83:051114
- [94] Bandyopadhyay M, Segal D. 2011. Quantum heat transfer in harmonic chains with self consistent reservoirs: Exact numerical simulations. *Phys. Rev. E* 84:011151
- [95] Sääskilähti K, Oksanen J, Tulkki J. 2013. Thermal balance and quantum heat transport in nanostructures thermalized by local langevin heat baths. *Phys. Rev. E* 88:012128
- [96] Velizhanin KA, Wang H, Thoss M. 2008. Heat transport through model molecular junctions: A multilayer multiconfiguration time-dependent hartree approach. *Chem. Phys. Lett.* 460:325–330
- [97] Saito K, Kato T. 2013. Kondo signature in heat transfer via a local two-state system. *Phys. Rev. Lett.* 111:214301
- [98] Boudjada N, Segal D. 2014. From dissipative dynamics to studies of heat transfer at the nanoscale: Analysis of the spin-boson model. *J. Phys. Chem. A* 118:11323–11336
- [99] Büttiker M. 1986. Role of quantum coherence in series resistors. *Phys. Rev. B* 33:3020–3026
- [100] Bolsterli M, Rich M, Visscher WM. 1970. Simulation of nonharmonic interactions in a crystal by self-consistent reservoirs. *Phys. Rev. A* 1:1086–1088
- [101] Rich M, Visscher WM. 1975. Disordered harmonic chain with self-consistent reservoirs. *Phys. Rev. B* 11:2164–2170
- [102] Bonetto F, Lebowitz JL, Lukkarinen J. 2004. Fourier’s law for a harmonic crystal with self-consistent stochastic reservoirs. *J. Stat. Phys.* 116:783–813
- [103] Visscher WM, Rich M. 1975. Stationary nonequilibrium properties of a quantum-mechanical lattice with self-consistent reservoirs. *Phys. Rev. A* 12:675–680
- [104] Neto AF, Lemos HCF, Pereira E. 2007. Heat conduction in quantum harmonic chains with alternate masses and self-consistent thermal reservoirs. *Phys. Rev. E* 76:031116
- [105] Pereira E, Lemos HCF, Avila RR. 2011. Ingredients of thermal rectification: The case of classical and quantum self-consistent harmonic chains of oscillators. *Phys. Rev. E* 84
- [106] Pereira E. 2010. Thermal rectification in quantum graded mass systems. *Phys. Lett. A* 374:1933–1937
- [107] Schwinger J. 1961. *J. Math. Phys.* 2:407–432
- [108] Kadanoff LP, Baym GA. 1962. Quantum statistical mechanics. Benjamin
- [109] Keldysh LV. 1965. *Sov. Phys. JETP* 20:1018
- [110] Haug H, Jauho AP, Cardona M. 2008. Quantum kinetics in transport and optics of semiconductors, vol. 2. Springer Berlin
- [111] Meir Y, Wingreen NS. 1992. Landauer formula for the current through an interacting electron region. *Phys. Rev. Lett.* 68:2512–2515
- [112] Velizhanin KA, Thoss M, Wang H. 2010. Meir–wingreen formula for heat transport in a spin-boson nanojunction model. *J. Chem. Phys.* 133:084503
- [113] Wang JS, Wang J, Zeng N. 2006. Nonequilibrium green’s function approach to mesoscopic thermal transport. *Phys. Rev. B* 74:033408
- [114] Rammer J. 2007. Quantum field theory of non-equilibrium states. Cambridge University Press
- [115] Xu Y, Wang JS, Duan W, Gu BL, Li B. 2008. Nonequilibrium green’s function method for phonon-phonon interactions and ballistic-diffusive thermal transport. *Phys. Rev. B* 78:224303
- [116] Luisier M. 2012. Atomistic modeling of anharmonic phonon-phonon scattering in nanowires. *Phys. Rev. B* 86:245407
- [117] Wang JS, Zeng N, Wang J, Gan CK. 2007. Nonequilibrium green’s function method for thermal transport in junctions. *Phys. Rev. E* 75:061128
- [118] Park TH, Galperin M. 2011. Self-consistent full counting statistics of inelastic transport. *Phys. Rev. B* 84:205450
- [119] Mingo N. 2006. Anharmonic phonon flow through molecular-sized junctions. *Phys. Rev. B* 74:125402
- [120] Thingna J, García-Palacios JL, Wang JS. 2012. Steady-state thermal transport in anharmonic systems: Application to molecular junctions. *Phys. Rev. B* 85:195452
- [121] Zhang L, Thingna J, He D, Wang JS, Li B. 2013. Nonlinearity enhanced interfacial thermal conductance and rectification. *Europhys. Lett.* 103:64002
- [122] Mingo N, Stewart D, Broido D, Lindsay L, Li W. 2014. In *Length-Scale Dependent Phonon Interactions*. Springer New York, 137–173
- [123] Agarwalla BK. 2013. Study of full-counting statistics in heat transport in transient and steady state and quantum fluctuation theorems. Ph.D. thesis, National University of Singapore
- [124] Li H, Agarwalla BK, Li B, Wang JS. 2013. Cumulants of heat transfer across nonlinear quantum systems. *Euro. Phys. J. B* 86:1–8
- [125] Breuer HP, Petruccione F. 2002. The theory of open quantum systems. Oxford university press
- [126] Nitzan A. 2006. Chemical dynamics in condensed phases: Relaxation, transfer and reactions in condensed molecular systems. Oxford University Press
- [127] Thingna J, Zhou H, Wang JS. 2014. Improved Dyson series expansion for steady-state quantum transport beyond the weak coupling limit: Divergences and resolution. *J. Chem. Phys.* 141
- [128] Buldum A, Leitner DM, Ciraci S. 1999. Thermal conduction through a molecule. *Europhys. Lett.* 47:208
- [129] Fujisaki H, Zhang Y, Straub JE. 2011. Non-markovian theory of vibrational energy relaxation and its applications to biomolecular systems. John Wiley and Sons, Inc., 1–33
- [130] Leitner DM. 2001. Vibrational energy transfer and heat conduction in a one-dimensional glass. *Phys. Rev. B* 64:094201
- [131] Yu X, Leitner DM. 2003. Vibrational energy transfer and heat conduction in a protein. *J. Phys. Chem. B* 107:1698–1707

- [132] Yu X, Leitner DM. 2005. Heat flow in proteins: Computation of thermal transport coefficients. *J. Chem. Phys.* 122:054902
- [133] Fujisaki H, Straub JE. 2005. Vibrational energy relaxation in proteins. *Proc. Natl. Acad. Sci. USA* 102:6726–6731
- [134] Weiss U. 1999. Quantum dissipative systems. World Scientific Singapore
- [135] Dekker H. 1987. Noninteracting-blip approximation for a two-level system coupled to a heat bath. *Phys. Rev. A* 35:1436–1437
- [136] Segal D. 2014. Heat transfer in the spin-boson model: A comparative study in the incoherent tunneling regime. *Phys. Rev. E* 90:012148
- [137] Yang Y, Wu CQ. 2014. Quantum heat transport in a spin-boson nanojunction: Coherent and incoherent mechanisms. *Europhys. Lett.* 107:30003
- [138] Segal D, Millis AJ, Reichman DR. 2010. Numerically exact path-integral simulation of nonequilibrium quantum transport and dissipation. *Phys. Rev. B* 82:205323
- [139] Wang C, Ren J, Cao J. 2014. Nonequilibrium energy transfer at nanoscale: A unified theory from weak to strong coupling. *arXiv1410.4366*
- [140] Taylor E, Segal D. 2015. Quantum bounds on heat transport through nanojunctions. *Phys. Rev. Lett.* 114:220401
- [141] Leggett AJ, Chakravarty S, Dorsey AT, Fisher MPA, Garg A, Zwerger W. 1987. Dynamics of the dissipative two-state system. *Rev. Mod. Phys.* 59:1–85
- [142] Makri N, Makarov DE. 1994. Tensor propagator for iterative quantum time evolution of reduced density matrices. i. theory. *J. Chem. Phys.* 102:4600–4610
- [143] Makri N, Makarov DE. 1995. Tensor propagator for iterative quantum time evolution of reduced density matrices. ii. numerical methodology. *J. Chem. Phys.* 102:4611–4618
- [144] Thoss M, Wang H, Miller WH. 2001. Self-consistent hybrid approach for complex systems: Application to the spin-boson model with debye spectral density. *J. Chem. Phys.* 115:2991–3005
- [145] Egger R, Weiss U. 1992. Quantum monte carlo simulation of the dynamics of the spin-boson model. *Z. Phys. B Condensed Matter* 89:97–107
- [146] Segal D. 2013. Qubit-mediated energy transfer between thermal reservoirs: Beyond the markovian master equation. *Phys. Rev. B* 87:195436
- [147] Carrega M, Solinas P, Braggio A, Sasseti M, Weiss U. 2015. Functional integral approach to time-dependent heat exchange in open quantum systems: general method and applications. *New J. Phys.* 17:045030
- [148] Wang JS. 2007. Quantum thermal transport from classical molecular dynamics. *Phys. Rev. Lett.* 99:160601
- [149] Liu R, Wang L. 2015. Thermal vibration of a single-walled carbon nanotube predicted by semiquantum molecular dynamics. *Phys. Chem. Chem. Phys.* 17:5194–5201
- [150] Turney JE, McGaughey AJH, Amon CH. 2009. Assessing the applicability of quantum corrections to classical thermal conductivity predictions. *Phys. Rev. B* 79:224305